Diesel Combustion Analysis Based on Two-Zone Model*
(Comparison between Model Analysis and Experiment)

Masahiro ISHIDA**, Hironobu UEKI**, Noboru MATSUMURA***, Masanori YAMAGUCHI**** and Gui-Feng LUO**

The proposed two-zone model of diesel combustion consists of a burned zone and an unburned zone, and the thermodynamic process is independent and adiabatic in each zone except that the air is entrained from the unburned zone to the burned zone under a specified condition of the excess air ratio during the combustion period. The excess air ratio in the diffusion combustion period is assumed to be constant in the present model. The calculated time histories of the burned-zone gas temperature and the cumulative soot formation were compared with the measured time histories of the flame temperature and the *KL* value based on the infrared two-color method. The calculated results agree qualitatively and partly quantitatively with the experimental results except for the swirl effect. As a result, it is shown that the present two-zone model analysis is very useful and effective in evaluating the combustion process in a DI diesel engine.

Key Words: Diesel Engine, Combustion Analysis, Two-Zone Model, Two-Color Method, Flame Temperature, Soot Concentration

1. Introduction

The simplest analysis of diesel combustion is the one-dimensional heat release analysis in which it is assumed that the combustion chamber is filled with a homogeneous gas. This one-zone model is, however, not suitable for the NO_x and soot formation analyses because they are significantly affected by the local temperature and the local excess air ratio in and around the fuel spray. Therefore, a stochastic one-zone model was proposed by Ikegami et al.[1], in which the heterogeneity of the in-cylinder gas, turbulence generation and turbulent mixing of fuel and air were taken into consideration.

A two-zone model consisting of an unburned zone and a heterogeneous flame zone was proposed by Kamimoto et al.[2]. The liquid-phase fuel, the unburned fuel-air mixture and the burned gas were included in the flame zone. In the analysis, the time history of excess air ratio of the flame zone was estimated using the measured combustion pressure and the flame temperature measured by the two-color method. Simpler two-zone models were proposed by Morel and Keribar[3] and Hatakeyama[4]. Their models consisted of an unburned gas zone and a uniform burned gas zone in which multiple flame zones were concentrated into a single burned zone. It was assumed that the gas is uniform in each zone and its thermodynamic state changes independently and adiabatically with the same pressure. The gas temperature of the burned zone was calculated using a simplified law for the air entrainment between two zones. A multizone model was proposed by Hiroyasu et al.[5] in which the fuel spray was divided into many elements and the processes of fuel evaporation, air entrainment, ignition and combustion were calculated in each element. These combustion models were proposed in accordance with specific research objectives.

The authors have proposed a two-zone combustion model in the present paper to clarify the

* Received 13th February, 1995. Japanese original: Trans. Jpn. Soc. Mech. Eng., Vol. 60, No. 573, B (1994), pp. 1845 1851. (Received 17th June, 1993)
** Faculty of Engineering, Nagasaki University, 1-14 Bunkyo machi, Nagasaki 852, Japan
*** Mantech Co., Ltd., 2-16-1 Shinbashi, Minato-ku, Tokyo 105, Japan
**** Hino Motor Corp., 3-1-1 Hinodai, Hino 191, Japan

formation processes of NO and soot in a diesel engine. The present two-zone model is somewhat similar to the model by Hatakeyama[4] in its fundamental assumptions and is somewhat similar to the model by Kamimoto et al.[2] in the method used to analyze the experimental data. It is, however, significantly different from those models in that the excess air ratio of the burned zone was determined through iterative calculation to obtain agreement between the NO_x concentrations obtained by the analysis and the experiment. In the analysis, the time histories of gas temperature in the burned zone, the NO formation rate and the rates of soot formation and soot oxidation were calculated on the basis of the experimental combustion pressure history. Furthermore, the calculated cumulative soot quantity was made equal to the measured exhaust soot quantity through another iterative calculation.

It is difficult to estimate the soot formation rate precisely using the simple two-zone model because, as is well known, it is dependent strongly on the local conditions of gas temperature, excess air ratio, swirl and squish. However, the NO formation rate is mainly dominated by the peak gas temperature during the first half of the combustion period, and the soot oxidation rate is mainly dominated by the gas temperature level during the second half. Therefore, emphasis was placed on the estimation of excess air ratio in the burned zone, which dominates the burned gas temperature. It will be shown that the burned gas temperatures calculated using the present two-zone model agree well with the experimental results measured by the two-color method[6],[7]. It is concluded that NO formation and soot formation processes can be accurately evaluated using the present two-zone model based on the assumption of a constant excess air ratio during the diffusion combustion period.

2. Combustion Analysis Model

2.1 Two-zone model

Figure 1 shows the concept of the present two-zone model. The fundamental assumptions of the two-zone model are as follows.

(1) The in-cylinder gas region is divided into two zones which consist of a burned zone and an unburned zone. The gas in each zone is considered to be uniform and its thermodynamic state changes independently and adiabatically with the same pressure.

(2) The weight of gas in the burned zone is the sum of the weights of the burned fuel and the entrained air, and other components such as the unburned fuel and the residual gas are included in the unburned zone. The weight of burned fuel is estimated from the cumulative heat release divided by the net calorific value of the fuel. Since the heat release rate is calculated from the experimental pressure history in the present analysis, the weight of burned fuel will be underestimated because heat loss occurs by convection and radiation during the combustion period. It seems, however, reasonable to estimate the weight of burned fuel from the heat release rate because the adiabatic process is assumed in the model and the heat loss does not contribute to increase of the combustion gas temperature.

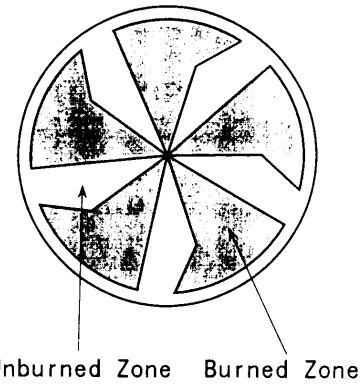

Fig. 1 Conceptualized two-zone model

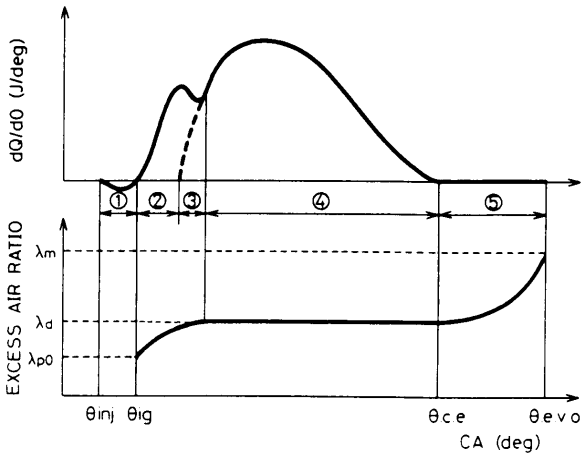

Fig. 2 Relationship between heat release curve and excess air ratio in burned zone

With respect to the amount of air entrained into the burned zone, a simple process of excess air ratio variation with crank angle is assumed in the heat release curve as shown in Fig. 2: the first period is ignition delay, the second is the premixed combustion period, the third is the premixed and diffusion combustion period and the fourth is the diffusion combustion period. The special feature of the present model is that the excess air ratio λ_d in the diffusion combustion period is assumed to be constant while the excess air ratio changes from λ_{p0} to λ_d continuously during the premixed combustion period in accordance with a specified parabolic function. The value of λ_{p0} is

basically assumed to be 1.0. After the diffusion combustion period, the excess air ratio varies from λ_d to λ_m which is defined as the mean excess air ratio in the cylinder. It seems reasonable to assume for simplicity that the mixing process occurs with the parabolic relationship, considering that the burned gas expands and diffuses gradually into the unburned zone and both gases mix with each other until the exhaust valve opening.

2.2 Analysis method and calculation procedure

2.2.1 Calculation of heat release rate The rate of heat release $dQ/d\theta$ is calculated from the measured combustion pressure P and the combustion chamber volume V using Eq. (1), which is derived from the one-dimensional heat balance analysis, and it is used for calculating the fuel weight burned per unit time. The in-cylinder mean gas temperature T_c is calculated using the equation of state (2).

$$dQ/d\theta = A/(k-1)\cdot\{kP\cdot dV/d\theta + V\cdot dP/d\theta\} \quad (1)$$

$$T_c = PV/G_cR \quad (2)$$

In the above equations, A denotes the reciprocal of the mechanical equivalent of heat, k denotes the ratio of specific heats which is a function of the in-cylinder averaged gas temperature and excess air ratio, and the gas constant R is a function of gas compositions.

2.2.2 Calculations of gas weight and in-cylinder mean excess air ratio The total in-cylinder gas weight $G_c(\theta)$ at any crank angle θ is, as shown by Eq. (3), the sum of the inducted air weight G_a, the residual gas weight G_f and the injected fuel weight $G_i(\theta)$ calculated from the cumulative reduced injection rate. The reduced injection rate is obtained from the actual injection rate by multiplying the ratio of the burned fuel weight corresponding to the cumulative heat release and the actually injected fuel weight. The gas weights $G_b(\theta)$ and $G_u(\theta)$ in the burned zone and the unburned zone are calculated by Eqs. (4) and (5) respectively, where $G_f(\theta)$ is the burned fuel weight derived from the cumulative heat release, L_{th} is the theoretical air quantity and $\lambda(\theta)$ is the excess air ratio.

$$G_c(\theta) = G_a + G_r + G_i(\theta) \quad (3)$$

$$G_b(\theta) = \{1+\lambda(\theta)L_{th}\}G_f(\theta) \quad (4)$$

$$G_u(\theta) = G_c(\theta) - G_b(\theta) \quad (5)$$

Figure 3 schematically shows the change in the gas weights with crank angle. The mean excess air ratios λ_0 before fuel injection and λ_m after finishing fuel injection are evaluated using the following equations.

$$\lambda_0 = G_{ab}/(G_{rb}L_{th}) \quad (6)$$

$$\lambda_m = (G_a+G_r)/(G_fL_{th}) \quad (7)$$

where:

$$G_{ab} = G_a + G_r(1-G_f/G_a),\quad G_{rb} = G_r(G_f/G_a).$$

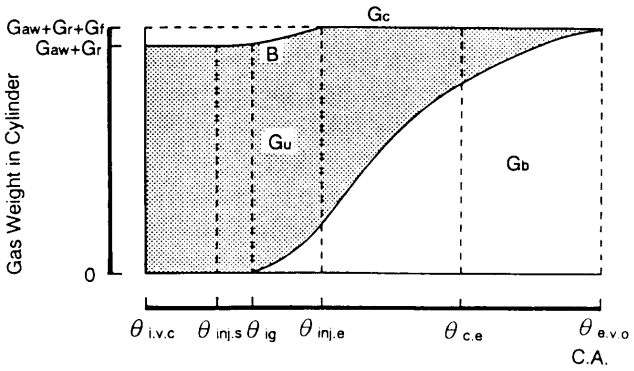

Fig. 3 Schematic change in gas weights with crank angle

2.2.3 Calculation of gas temperature The in-cylinder mean gas temperature is calculated using Eq. (2), while the gas temperature T_u in the unburned zone is calculated using Eq. (8) based on the isentropic relation. The gas temperature T_b in the burned zone is calculated using Eq. (9) derived from the internal energy balance in the cylinder, and the gas volume V_b of the burned zone is calculated using Eq. (10) based on the equation of state.

$$T_u = T_0\{P/P_0\}^{(k-1)/k} \quad (8)$$

$$T_b = (G_cc_{vc}T_c - G_uc_{vu}T_u)/G_bc_{vb} \quad (9)$$

$$V_b = G_bR_bT_b/P \quad (10)$$

In the above equations, P_0 and T_0 denote the in-cylinder pressure and the in-cylinder mean gas temperature before ignition, respectively. The ratio of specific heats k is a function of T_u and λ_0. c_{vc}, c_{vu} and c_{vb} are the specific heats at constant volume in the cylinder, in the unburned zone and in the burned zone, respectively, and they are a function of the temperature and the excess air ratio in the respective zone.

2.2.4 Calculation of NO formation rate It is well known that the NO_x concentration in the exhaust gas cannot be predicted by chemical equilibrium composition analysis because of a slow reaction rate of NO. The NO formation rate (mole/cm^3/s) is, therefore, calculated using the following equation derived from the extended Zel'dovich mechanism, in which nine chemical equilibrium mole concentrations[8], namely [CO], [CO_2], [O_2], [H_2], [H_2O], [OH], [H], [O] and [N_2] are taken into consideration but not [NO].

$$\frac{\Delta[\mathrm{NO}]}{\Delta t} = a\{k_1[\mathrm{N_2}][\mathrm{O}] - b[\mathrm{NO}]^2\} \quad (11)$$

$$a = \frac{2(k_2[\mathrm{O_2}]+k_3[\mathrm{OH}])}{r_1[\mathrm{NO}]+k_2[\mathrm{O_2}]+k_3[\mathrm{OH}]}$$

$$b = \frac{r_1r_2[\mathrm{O}]+r_1r_3[\mathrm{H}]}{k_2[\mathrm{O_2}]+k_3[\mathrm{OH}]}$$

where r_1, r_2, r_3, k_1, k_2 and k_3 are the reaction rate constants which are given in Ref. (9).

2.2.5 Calculation of soot formation and oxidation rates The net soot formation rate is estimated using model equations proposed by Morel and

Keribar[3] in which the soot formation rate $(dS/dt)_f$ is calculated using Eq. (12), the soot oxidation rate $(dS/dt)_b$ using Eq. (13) and the net soot formation rate $(dS/dt)_n$ using Eq. (14).

$$(dS/dt)_f = A_1 m_d \exp(-A_2/T_b) \quad (12)$$

$$(dS/dt)_b = (B_1 S/\rho_s d_s)\cdot\exp(-B_2/T_{rad})\sqrt{P_{02}} \quad (13)$$

$$(dS/dt)_n = (dS/dt)_f - (dS/dt)_b \quad (14)$$

S denotes the cumulative soot quantity (kg). m_d is the mass rate of diffusion combustion (kg/s) which is estimated from the approximate heat release curve in the diffusion combustion period as shown in Fig. 2. T_b is the gas temperature in the burned zone determined by the present two-zone model analysis. ρ_s is the density of soot particles ($=9\,000$ kg/m^2) and d_s is the diameter of soot particles (m). P_{02} is the partial pressure of O_2 in the burned zone (kg/m^2). Several constants in the equations are set as follows: $A_1=0.3$, $A_2=3\,000$, $B_1=0.19$, $B_2=10\,000$. T_{rad} is the radiation temperature of the burned gas defined in Ref. (3).

2.2.6 Calculation procedure

(i) The following measured data are required as the initial conditions in the present analysis: the suction air pressure and temperature, the time histories of the in-cylinder pressure, the fuel injection pressure and the nozzle needle valve lift, the rates of specific fuel consumption and specific air consumption, and the NO_x concentration and smoke density in the exhaust gas in addition to the engine specifications and the engine running conditions.

(ii) An initial value of the excess air ratio in the diffusion combustion period λ_d is assumed.

(iii) The gas weight and the temperature in each zone are calculated for every crank angle using Eqs. (2)-(9). After calculating ten chemical equilibrium mole concentrations of the burned-zone gas, the NO formation rate (mol/cm^3/deg.) is estimated by applying the Runge-Kutta method to Eq. (11). The unit of NO formation rate shown in the following figures is mol/deg., which is the product of the rate calculated using Eq. (11) and the burned-zone volume V_b based on Eq. (10).

(iv) The NO concentration (ppm) in the exhaust gas is calculated by considering the gas volume from the cumulative NO formation which is obtained by integrating the NO formation rate during the combustion period. Comparing the calculated NO concentration with the measured NO_x concentration in the exhaust gas, the calculation is repeated until a good agreement is obtained between the analysis and the experiment by correcting the assumed excess air ratio λ_d of the diffusion combustion period.

(v) The converged value λ_{d0} of the diffusion combustion excess air ratio is determined through iterative calculation, then the time history of the burned-zone gas temperature can be determined.

(vi) The rates of soot formation, oxidation and net formation are calculated from Eqs. (12), (13) and (14) using the determined burned-zone gas temperature. Calculation is repeated until a good agreement is obtained between the analytical cumulative soot formation and the experimental smoke data in the exhaust gas by correcting the equivalent soot particle diameter d_s. Meanwhile, the mass rate of diffusion combustion m_d is given by the heat release curve approximated by the Wiebe function[10] during the diffusion combustion period as shown in Fig. 2.

2.2.7 Example calculation using two-zone model

An example of the analytical result using the present two-zone model is shown by the solid line in Fig. 4. In the figure, another analytical result which was calculated using the excess air ratio pattern indicated in the Ref. (4) is shown by the dashed line. By comparing the two results, it becomes clear that the burned-zone gas temperatures are significantly different from each other, and the burned-zone gas temperature based on the air entrainment law shown in Ref. (4) is too high in the first half and too low in the second half of the combustion process compared with the experimental temperature history shown later. A similar analytical result was reported in the Ref. (11). The models in

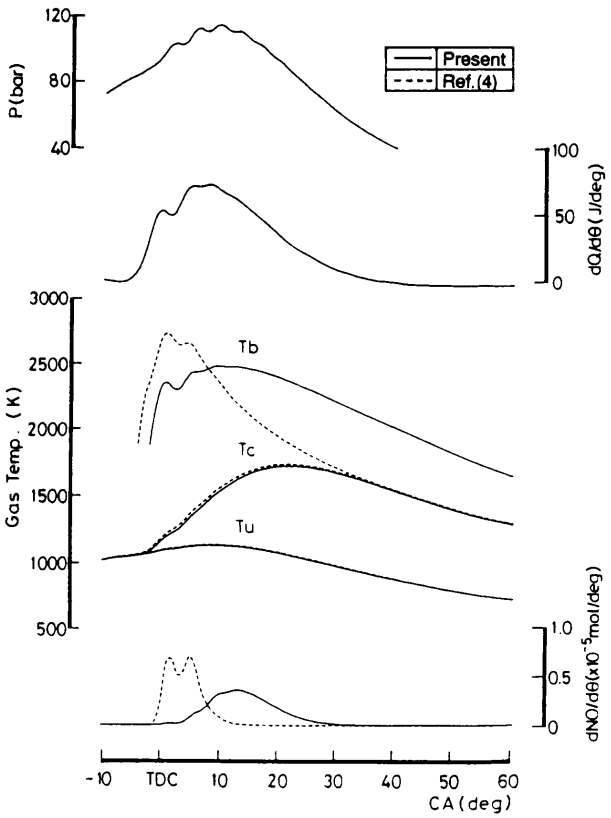

Fig. 4 Example calculated using two zone model analysis

Refs. (4) and (11) give too low burned-zone gas temperature due to equalization of gas temperatures between the burned-zone and the in-cylinder average at the end of the diffusion combustion period.

3. Comparison between Experiment and Analysis

3.1 Test engine and measuring system

The test engine is a four-cylinder high-speed turbocharged direct-injection diesel engine with an intercooler for automobile, namely type 4D31-T manufactured by Mitsubishi Motor Corporation. It has a bore of 100 mm, a stroke of 105 mm, a compression ratio of 16 and a maximum output of 95.6 kW (130 PS)/3 500 rpm. The test fuel is ordinary gas oil with a cetane index of about 55. For measuring the time histories of the flame temperature and the soot concentration, a beveled-edge light-pipe sensor was used. The sensor was inserted into the combustion chamber through the glow plug hole of the engine and the measurement volume is shown by the hatched region in Fig. 5, in which the fuel spray axes are also shown by the five arrowheaded lines. The flame temperature measuring system[6] consisted of the light-pipe sensor, an optical fiber cable about 20 m long, the optical fiber thermometer Model 100 manufactured by Accufiber Corp., the four-channel combustion analyzer Model CB-466 manufactured by Ono Sokki Co. Ltd. and a personal computer. Two infrared wavelengths of 950 and 800 nm were used in this system for the two-color method.

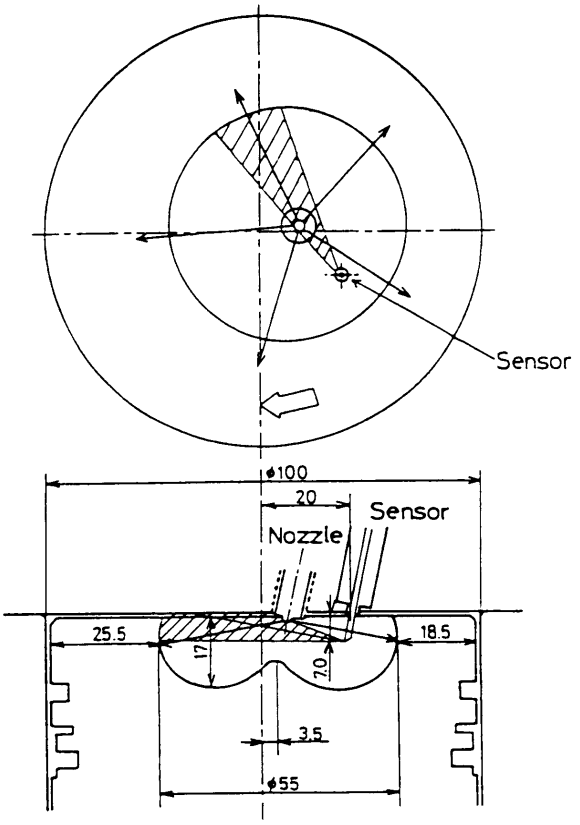

Fig. 5 Measurement volume and fuel spray axes

The measured flame temperature T_f can be considered to be the temperature of soot or solid carbon particles in the burned zone which have almost the same temperature as the burned gas, and it is compared with the burned-zone gas temperature calculated by the present two-zone model analysis in Figs. 6 to 8. It should be pointed out before comparing both temperatures that the calculated temperature is assumed to be uniform throughout the burned zone, while the experimental one is not uniform throughout the measurement volume. Temperature measurement error may occur in the initial combustion period due to the heterogeneity in the measurement volume in which the liquid-phase fuel and the vapor-phase fuel are present in addition to the burning gas. It is considered, however, that this error becomes small in the second half of the combustion period because the measurement volume is then filled with the burned gas which has an almost uniform temperature.

3.2 Comparison between measured and calculated results

Figures 6 to 8 show comparisons between the experiment and the analysis for the time histories of gas temperature and soot in the burned zone. In these figures, $dQ/d\theta$ is the experimental heat release rate

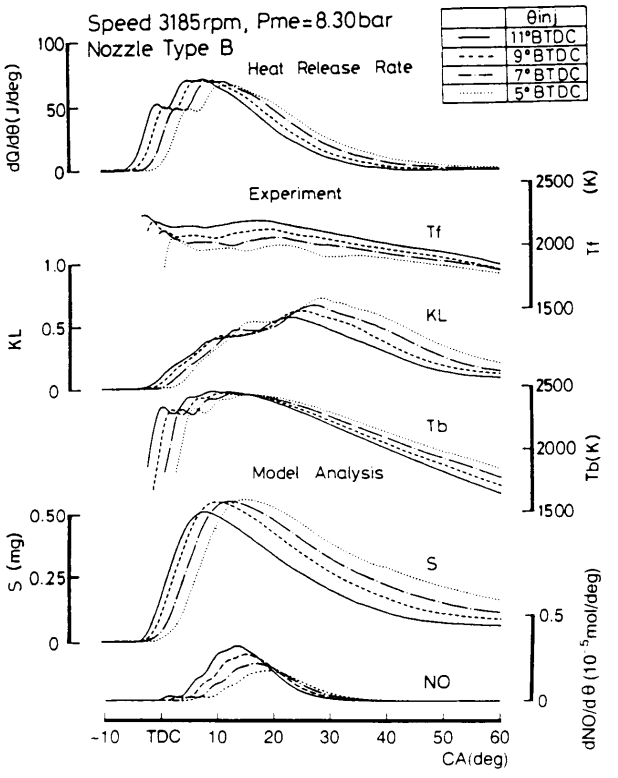

Fig. 6 Comparison between experiment and analysis (Injection timing retard; 3 185 rpm)

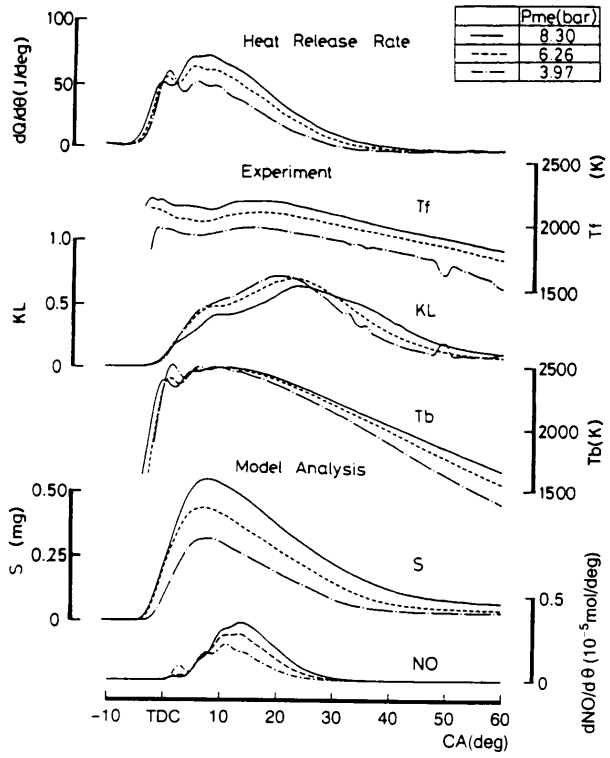

Fig. 7 Comparison between experiment and analysis (Mean effective pressure variation ; 3 185 rpm)

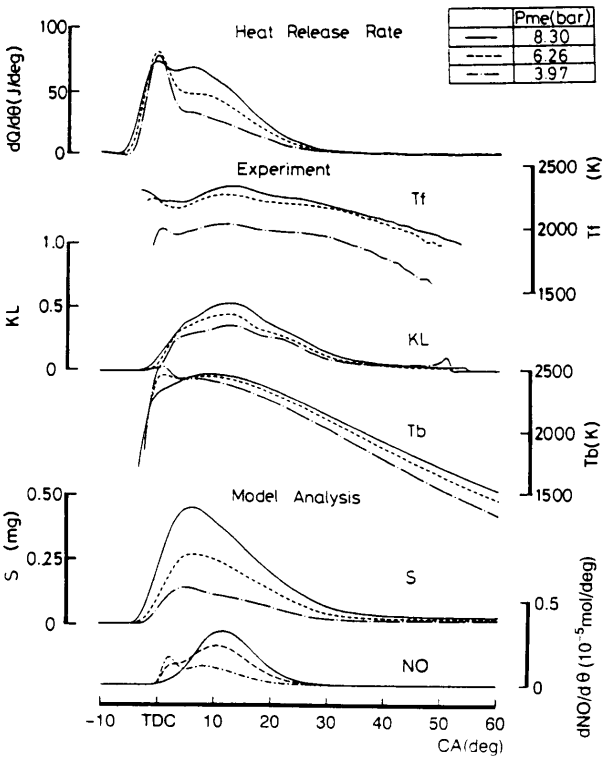

Fig. 8 Comparison between experiment and analysis (Mean effective pressure variation ; 1 750 rpm)

calculated from the measured combustion pressure history, T_f is the experimental flame temperature and KL is the soot concentration parameter measured simultaneously by the two-color method. T_b is the calculated burned-gas temperature, S is the cumulative soot formation and $dNO/d\theta$ is the NO formation rate calculated using the present two-zone model. Figure 6 shows the results in the case of injection timing retard from 11 to 5 deg BTDC for the engine speed of 3 185 rpm and the brake mean effective pressure P_{me} of 8.30 bar. Figures 7 and 8 show the results in the case that P_{me} was decreased from 8.30 to 3.97 bar while keeping the engine speed constant at 3 185 or 1 750 rpm, respectively. The measured time histories of the experimental results are the mean values of continuous measurement over 360 cycles.

3. 2. 1 Analysis on injection timing retard The temperature histories of T_b and T_f seem to be quite different in both time histories in which the peak temperature occurs at different crank angles. However, the relative shift of the peak temperature position, the decreases in the level of the maximum temperature and in the temperature level at the end of combustion due to timing retard show the same tendency in both experiment and analysis although the temperature in the initial combustion period is lower in the experiment than in the analysis. For instance, for the injection timing of 11 deg BTDC, the experimental peak temperature is 2 250 K near the 15 deg crank angle, while the calculated one is 2 450 K near the 10 deg crank angle. Yan and Borman[12] obtained a temperature as high as that in the present calculation in their experimental data measured in a larger test engine by the visible two-color method.

Why is the measured flame temperature lower than the calculated one in the initial combustion period? One of the reasons is that the temperature measured by the infrared two-color method has a tendency to be slightly lower than that measured by the visible two-color method as was shown by Matsui et al.[13]. Another reason may be the influence of the heterogeneity in the measurement volume or the optical path as mentioned above. The influence of the radiation reflected from the opposite walls may also be significant. In addition to these reasons, judging from the result that the measured temperature fluctuation was ± 200 K from cycle to cycle in the initial combustion period[7] as well as the finding that the temperature shows a minimum near the crank angle of 5 to 10 deg which corresponds to the end of fuel injection, the flame temperature in the initial combustion period might actually be as high as the calculated burned-gas temperature.

Table 1 shows the comparison between the calculated temperature of the burned zone T_b and the experimental one T_f at the combustion end crank angle θ_{ce} in the cases of timing retard from 11 to 5 deg

Table 1 Comparison of temperatures at combustion end between experiment and analysis

θ inj (deg.BTDC)	11	9	7	5
θ ce (deg.ATDC)	40	45	52	66
Tb (K)	2010	1960	1900	1840
Tf (K)	2000	1920	1850	1770

BTDC. These T_b and T_f agree quantitatively with each other although the measurement volume was fixed in the upper part of the combustion chamber during the piston downstroke. This is because the temperature becomes almost uniform in the measurement volume judging from the calculation that the burned-zone volume covers about 70% of the combustion chamber at the end of the diffusion combustion period. Furthermore, judging from the result that the calculated burned-zone temperature has a tendency to decrease more rapidly than the experimental flame temperature after the end of the diffusion combustion period, the gas mixing rate between the burned zone and the unburned zone is slightly slower in the experimental process compared with the rate specified in the present analysis.

The experimental KL curve shows two peaks, and the first one near the crank angle of 10 deg ATDC coincides well with the peak position of the calculated soot formation curve. However, no second peak is obtained in the analysis because the swirl effect is not taken into consideration in the present two-zone model. The second and highest peak near the crank angle of 25 deg ATDC in the KL curve might be caused by the interaction between two adjacent spray flames due to the swirl flow in the cylinder. Macroscopically, the results of experiment and analysis for the relative delay of the peak position due to timing retard are in good agreement, and the observed increase in KL due to timing retard at the end of combustion agrees qualitatively with the result of analysis. The same phenomenon due to the swirl flow is seen in Fig. 7 as well as in Fig. 6 under the same engine speed condition.

3. 2. 2 Analysis on mean effective pressure variation As shown in Figs. 7 and 8, the measured flame temperature was decreased significantly with decreasing P_{me} throughout the entire combustion period. On the other hand, the calculated temperature of the burned zone is decreased with P_{me} only after reaching the peak temperature. It is notable that the two-zone model analysis shows nearly equal peak temperatures even under different P_{me} conditions. The temperature measured by the two-color method might be affected by the heterogeneity in the measurement volume, as mentioned before in connection with Fig. 6. The fuel-air mixture condition in the fuel spray varies with P_{me} due to the changes in the fuel injection quantity and the injection pressure.

In both Figs. 7 and 8, the experimental KL value in the second half of the combustion period decreases with decreasing P_{me} because the combustion duration is shortened, and this phenomenon agrees well with the calculated result. According to Eqs. (12) and (13), soot formation occurs only in the combustion period, while the soot oxidation occurs even after the diffusion combustion period if the temperature is high enough to oxidize soot particles. It is clearly shown in both experiment and analysis that the soot oxidation process continues after the heat release rate becomes zero. This suggests that the mixing between the burned gas and the unburned gas occurs gradually after the diffusion combustion period.

The swirl effect on the KL curves is observed in Figs. 7 and 8 as well as in Fig. 6. Comparing Fig. 7 with Fig. 8, the swirl effect on the KL curve is more significant under the higher engine speed condition.

4. Conclusions

In order to estimate the combustion temperature and the NO formation rate in diesel combustion accurately, a two-zone model was proposed in the present paper. In this model, which consists of a burned zone and an unburned zone, it was assumed that the air is entrained from the unburned zone to the burned zone under a specified condition of excess air ratio. The special feature of the present model is that the excess air ratio of the burned zone is assumed to be constant during the diffusion combustion period and it is an unknown value which is determined through iterative calculation to obtain a good agreement in the NO_x concentrations between the analysis and the experiment. The calculated time histories of the burned-zone gas temperature and the cumulative soot formation are compared with the measured flame temperature and the KL value. The results obtained lead to the following conclusions.

(1) The calculated burned-zone gas temperature agreed qualitatively or partly quantitatively with the measured flame temperature in terms of the temperature level, the time history and the temperature variation with the engine running condition.

(2) It was found that the assumptions of the excess air ratio pattern and the constant excess air ratio during the diffusion combustion period were suitable for analyzing the combustion process in a DI diesel engine.

(3) The time history of the cumulative soot

formation agreed qualitatively with the *KL* history measured by the two-color method; however, the present two-zone model cannot predict the history of soot formation accurately because the swirl effect is not taken into consideration.

Acknowledgement

The authors express their gratitude to Mr. Z. L. Chen, Nagasaki University, and Mr. H. Kondo, Daihatsu Diesel Co. Ltd. for their assistance and support.

References

(1) Ikegami, M. Shioji, M., and Koike, M., A Stochastic Approach to Model the Combustion Process in Direct Injection Diesel Engines, Proc. of Twentieth Symposium (Int.) on Combustion, The Combustion Institute, (1984), p. 217.

(2) Kamimoto, T., Aoyagi, Y., Matsui, Y., and Matsuoka, S., The Effects of Some Engine Variables on Measured Rates of Air Entrainment and Heat Release in a DI Diesel Engine, SAE Trans., Paper No. 800253 (1980)

(3) Morel, T. and Keribar, R., Heat Radiation in D. I. Diesel Engine, SAE, Paper No. 860445 (1986)

(4) Hatakeyama, T., Predicting Nitric Oxide Formation in Direct Injection Diesel Engine, Technical Report of Mitsubishi Heavy Industries, (in Japanese), Vol. 12, No. 3 (1975), p. 341.

(5) Hiroyasu, H., Kadota, T. and Arai, M., Development and Use of Spray Combustion Modeling to Predict Diesel Engine Efficiency and Pollutant Emissions (Part 1, Part 2), Trans. Jpn. Soc. Mech. Eng., (in Japanese), Vol. 48, No. 432, B (1982), p. 1606 and p. 1614.

(6) Ishida, M., Matsumura, N., Ueki, H., Ito, G., Kubota, S. and Ko, J.G., Measurement of Diesel Combustion by Optical Fiber Thermometer (Part 1, Combustion Process and Exhaust Emission Level), Trans. Jpn. Soc. Mech. Eng., (in Japanese), Vol. 58, No. 555, B (1992), p. 3482.

(7) Ishida, M., Matsumura, N., Ueki, H., Ito, G., Yamaguchi, M. and Ko, J.G., Measurement of Diesel Combustion by Optical Fiber Thermometer (Part 2, Local Combustion Behavior in Combustion Chamber), Trans. Jpn. Soc. Mech. Eng., (in Japanese), Vol. 58, No. 555, B (1992), p. 3482.

(8) Mizutani, Y., Combustion Engineering, (in Japanese), (1991), p. 227, Morikita Publishing Co. Ltd.

(9) Formation Mechanisms and Suppression of Controls of Pollutants in Combustion System, Jpn. Soc. Mech. Eng., (1980), p. 51.

(10) Miyamoto, N., Chikahisa, T. Murayam, T., and Sawyer, R., Description and Analysis of Diesel Engine Rate of Combustion and Performance Using Wiebe's Functions, SAE, Paper No. 850107 (1985)

(11) Ishida, M., Izumi, S., Yoshimura, Y., Suetsugu, H. and Ueki, H., Studies on Combustion and Exhaust Emissions in a High Speed Diesel Engine (Part 1, Reduction in Exhaust NO_x), Trans. Jpn. Soc. Mech. Eng., (in Japanese), Vol. 54, No. 498, B (1988), p. 506.

(12) Yan, J. and Borman, G.L., Analysis and In-Cylinder Measurement of Particulate Radiant Emissions and Temperature in a Direct Injection Diesel Engine, SAE, Paper No. 881315 (1988)

(13) Matsui, Y., Kamimoto, T. and Matsuoka, S., A Study on the Application of the Two-Color Method to the Measurement of Flame Temperature and Soot Concentration in Diesel Engine, SAE-Trans., Paper No. 800970 (1980)